JOURNAL OF NEUROTRAUMA 35:842–853 (March 15, 2018)

DOI: 10.1089/neu.2017.5184

Rapamycin Exacerbates Cardiovascular Dysfunction after Complete High-Thoracic Spinal Cord Injury

Khalid C. Eldahan,[1,2] David H. Cox,[1] Jenna L. Gollihue,[1,2] Samir P. Patel,[1,2] and Alexander G. Rabchevsky[1,2]

Abstract

Autonomic dysreflexia (AD) is a potentially life-threatening syndrome in individuals with spinal cord injury (SCI) above the T6 spinal level that is characterized by episodic hypertension in response to noxious stimuli below the lesion. Maladaptive intraspinal plasticity is thought to contribute to the temporal development of AD, and experimental approaches that reduce such plasticity mitigate the severity of AD. The mammalian target of rapamycin (mTOR) has gained interest as a mediator of plasticity, regeneration, and nociceptor hypersensitivity in the injured spinal cord. Based on our preliminary data that prolonged rapamycin (RAP) treatment markedly reduces mTOR activity in the cord weeks after high-thoracic (T4) spinal transection, we sought to determine whether RAP could modulate AD development by impeding intraspinal plasticity. Naïve and injured rats were administered RAP or vehicle every other day, beginning immediately after injury for four weeks, and hemodynamic monitoring was conducted to analyze the frequency of spontaneously occurring AD, as well as the severity of colorectal distention (CRD) induced AD. Results showed that after SCI, RAP significantly exacerbated sustained body weight loss and caused a marked elevation in resting blood pressure, with average daily blood pressure rising above even normal naïve levels within one week after injury. Moreover, RAP significantly increased the frequency of daily spontaneous AD and increased the absolute blood pressure induced by CRD at three weeks post-injury. These dynamic cardiovascular effects were not, however, correlated with changes in the density of nociceptive c-fibers or c-Fos+ neurons throughout the spinal cord, indicating that intraspinal plasticity associated with AD was not altered by treatment. These findings caution against the use of RAP as a therapeutic intervention for SCI because it evokes toxic weight loss and exacerbates cardiovascular dysfunction perhaps mediated by increased peripheral nociceptor sensitivity and/or vascular resistance.

Keywords: autonomic; mammalian target of rapamycin; plasticity; sprouting; sympathetic

Introduction

In addition to loss of sensory and motor function, traumatic spinal cord injury (SCI) can also disrupt central autonomic pathways that are important for maintaining cardiovascular homeostasis. Autonomic dysreflexia (AD) is an abnormal hypertensive syndrome that presents in many individuals with SCI above the sixth thoracic (T6) spinal level—the majority of cases.[1] Injuries above this level segregate critical spinal sympathetic pre-ganglionic neurons (SPN) involved in blood pressure regulation from important vasomotor nuclei in the brainstem and hypothalamus, leaving them susceptible to unrestrained reflex activation by stimuli below the lesion level. Notably, SPNs below T6 control vasomotor tone of the extensive mesenteric vasculature, which accounts for approximately 30% of the total blood volume.[2,3]

Noxious distension of the bladder or bowel is among the most common triggers of AD,[4,5] although a variety of other noxious and non-noxious stimuli are also known to precipitate an event.[6,7] The AD is seen as episodic hypertension accompanied by baroreflex-mediated bradycardia, although tachycardia alternatively may be present.[5] While the severity of hypertension during an AD episode can vary widely, if not treated promptly and properly, then severe episodes can lead to stroke, hypertensive encephalopathy, seizures, cardiac arrest, and even death.[8–13]

A contributing factor to the development of AD is maladaptive plasticity of sympathetic reflex circuitry.[14] After transection SCI, the sprouting of unmyelinated afferent c-fibers carrying nociceptive signals from the pelvic viscera into the lumbosacral cord, as well as ascending propriospinal fibers that project rostrally and relay these signals toward SPNs in the thoracic cord, are associated temporally with the development of AD.[15–17] Moreover, the extent of nociceptive afferent fiber sprouting, which is dependent on injury-induced elevations in nerve growth factor,[15,18] positively correlates with the extent of mean arterial pressure (MAP) increases during

[1]Department of Physiology and [2]Spinal Cord and Brain Injury Research Center, University of Kentucky, Lexington, Kentucky.

AD induced experimentally through noxious colorectal distension (CRD).[15,16] While therapeutic strategies aimed at mitigating such maladaptive plasticity are attractive for their potential to prevent or reduce the development of AD, no such treatments exist in the clinical setting.

Recently, the mammalian target of rapamycin (mTOR) has gained considerable interest as a target to modulate post-traumatic plasticity within the central nervous system (CNS). Considered a ''master regulator'' of protein synthesis, mTOR is expressed ubiquitously in eukaryotic cells and integrates a variety of environmental cues such as nutrient availability and growth factors to coordinate important cellular processes such as cell growth, proliferation, and autophagy.[19–21] Several lines of evidence indicate that mTOR is also a critical mediator of neuronal sprouting and regeneration after neurotrauma.

After crush injury of the optic nerve in mice, deletion of phosphatase and tensin homologue (PTEN), a negative regulator of mTOR, promotes robust regeneration in an mTOR-dependent manner.[22] Genetic mouse models of enhanced mTOR activity after SCI via PTEN deletion in the motor cortex demonstrate increased regeneration and compensatory sprouting of injured descending corticospinal tract axons.[23,24] Moreover, pharmacological inhibition of mTOR signaling with rapamycin (RAP) after traumatic brain injury has been shown to decrease seizure frequency and associated maladaptive sprouting of hippocampal mossy fibers.[25] Together, these studies suggest that this highly conserved signaling pathway that is present in all mammalian cells[26] may also be involved in the sprouting of ascending afferent pathways underlying the development of AD.

In addition to its involvement in CNS structural plasticity, mTOR regulates nociceptive sensitivity in both the normal and injured states. In naïve rats, pharmacological blockade of spinal mTOR with RAP prevents the development of neuronal hyperexcitability and behavioral hypersensitization associated with pain induced by injection of formalin into the hindpaw.[27] In rats with cyclophosphamide-induced cystitis, a condition characterized by bladder hyperactivity and pelvic pain, RAP significantly reduces the expression of calcitonin gene related peptide (CGRP) and substance P in the spinal cord dorsal horn.[28] Further, inhibition of mTOR after SCI in rats treated with RAP attenuates the development of neuropathic pain in correlation with reduced expression of both CGRP and substance P, two neuropeptides involved in the regulation of nociceptive sensitivity.[29] Collectively, these studies suggest that mTOR is involved in the regulation of both intraspinal plasticity and nociceptor sensitivity, but it is unknown whether mTOR modulates the sprouting of sensory and/or propriospinal pathways after SCI in relation to the development of AD.

Therefore, in contrast to SCI studies attempting to promote sprouting and regeneration of descending corticospinal tracts by enhancing mTOR activity, we performed experiments to test how the inhibition of mTOR after complete high-thoracic SCI with RAP alters the temporal development of AD, and whether it modulates injury-induced maladaptive plasticity of primary afferent fibers and/or propriospinal neurons.

Methods

Collectively, a total of 33 age and sex-matched rats were used for all experiments, including $n=23$ for telemetric monitoring ($n=3$ naïve + vehicle, $n=3$ naïve + RAP, $n=7$ SCI + vehicle, $n=10$ SCI + RAP) and $n=10$ for Western blot analysis ($n=2$ naïve, $n=2$ 10 days post-injury [DPI], $n=2$ 21 DPI, $n=2$ 21 DPI + CRD, $n=2$ 21 DPI + CRD + RAP).

Cardiophysiological monitoring

All animal housing conditions, surgical procedures, and post-operative care were conducted according to the University of Kentucky Institutional Animal Care and Use Committee and the National Institutes of Health animal care guidelines. As described in detail,[30,31] seven days before SCI, naïve anesthetized (2% isoflurane) 3 to 3.5 month old female Wistar rats ($\sim$275 g, $n=23$) were implanted with telemetric blood pressure transmitters (model HD-S10, Data Sciences International, Inc., St. Paul, MN) into the descending aorta. The probes were secured to the abdominal wall with silk sutures before closing the skin with 3-0 polyglactin sutures and surgical staples. Animals were then treated post-operatively, as described below. Blood pressure was monitored 24/7 (500 Hz sampling rate) using the Dataquest A.R.T. acquisition system (Data Sciences International, Inc., St. Paul, MN) beginning two days pre-injury through four weeks post-injury. Rats were single-housed, with each cage placed directly on top of its corresponding data receiver plate (model RPC-1, Data Sciences International, Inc., St. Paul, MN).

Captured recordings were binned into 24-h segments for analysis of daily blood pressure, heart rate (HR), and spontaneous AD (sAD). As described previously in detail,[31] sAD was analyzed using a custom algorithm written and implemented in Matlab software (The MathWorks, Inc., Natick, MA). Briefly, this algorithm simultaneously processes 24-h MAP and HR traces for instances where a rise in MAP of 10 mm Hg or more above baseline is accompanied by a decrease in HR of at least 10 beats per minute (BPM). While this algorithm does not require such events to be sustained above baseline for a specific duration, it does require the rise in MAP over baseline to occur within a 35-sec window. The MAP rises that were accompanied by tachycardia (an increase in HR) were not included in these detections. From the computer automated AD event detections, a single human observer then manually eliminated false-positive results stemming from technical artifacts that can arise during normal rat movements and during planned CRD procedures.

Spinal cord transections

One week after telemetry probe implantation, 17 of 23 rats undergoing cardiophysiological monitoring were designated for the SCI groups. These randomly selected telemetry rats were anesthetized (ketamine, 80 mg/kg; xylazine 7 mg/kg intraperitoneally [IP]) and underwent a T3 laminectomy before complete transection of the T4 spinal cord (T4Tx) using a scalpel blade, as described previously.[16,31] In addition, 8 of 10 non-telemetered rats from the Western blot cohort were designated for T4Tx to examine the effect of RAP treatment on mTOR activity after SCI. Altogether, a total of 25 rats underwent T4Tx, including $n=17$ for telemetry experiments and $n=8$ for Western blot experiments.

Two independent observers confirmed complete spinal cord transection of each rat based on full separation of the rostral and caudal stumps. Immediately afterward, gelfoam was placed into the transection site to achieve hemostasis, and the overlying muscles were sutured with 3-0 polyglactin before stapling the skin with wound clips (Stoelting, Wood Dale, IL).

Post-operative care

All rats that underwent ketamine/xylazine anesthesia received IP injections of yohimbine (3.2 mg/kg Lloyd Laboratories, Shenandoah, IA) to reverse the effects of xylazine. Injured rats were then housed one per cage with food and water *ad libitum*. A heating pad was placed between each cage and its corresponding data receiver plate for the duration of the study period. Immediately post-operation, rats were administered 10 mL of lactated Ringer solution subcutaneously (SC). Post-surgical pain management was achieved with twice daily buprenorphine HCl injections (0.03 mg/kg SC;

Reckitt-Benckiser Pharmaceuticals Inc., Richmond, VA) for three days. All rats received two daily injections of the antibiotic cefazolin (33.3 mg/kg SC; WG Critical Care, LLC, Paramus, NJ) for five days after operation, and injured rats received twice daily manual bladder expression for two to three weeks or until they regained spontaneous bladder voiding reflexes without signs of urinary tract infection.

RAP administration and CRD

All rats were weighed before injections to ensure accurate drug dosage throughout the study period. Rapamycin (3 mg/kg, LC Labs, Woburn, MA) or vehicle (4% ethanol, 5% polyethylene glycol-400, 5% polysorbate-80 in 0.1M phosphate buffered saline [PBS]) was injected IP immediately after injury and then every other day until euthanasia at 10 and 21 DPI for the Western blot cohort, or 28 DPI for telemetered rats. In rodent SCI models, RAP has been administered at 6 mg/kg every other day,[32] 3 mg/kg daily,[33] or 1 mg/kg daily.[34] We chose a 3 mg/kg alternate day dosage based on optimal effectiveness in blocking mTOR signaling.[35] Moreover, we found that this dosage attenuates mTOR activity in the spinal cord after T4Tx, as assessed by phosphorylation of the downstream S6 ribosomal protein (Fig. 1).

On days 14, 21, and 28 post-SCI, naïve and injured rats undergoing telemetric monitoring underwent two consecutive trials of CRD using a balloon-tipped catheter (Swan-Ganz, model# 111F7, Edwards Lifesciences, Irvine, CA) inserted 2 cm into the rectum and secured to the tail with surgical tape, as described.[31] In addition, non-telemetered Western blot rats designated for SCI + CRD similarly underwent two consecutive CRD trials at 21 DPI before euthanasia and tissue collection. After catheterization, rats were placed into cylindrical plastic restrainers (Cat # 51335, Stoelting, Wood Dale, IL) to prevent them from tampering with the catheter. All rats were then left in a quiet and dark environment to acclimate to the catheter and restrainer for 30 min before balloon inflation and CRD measurements.

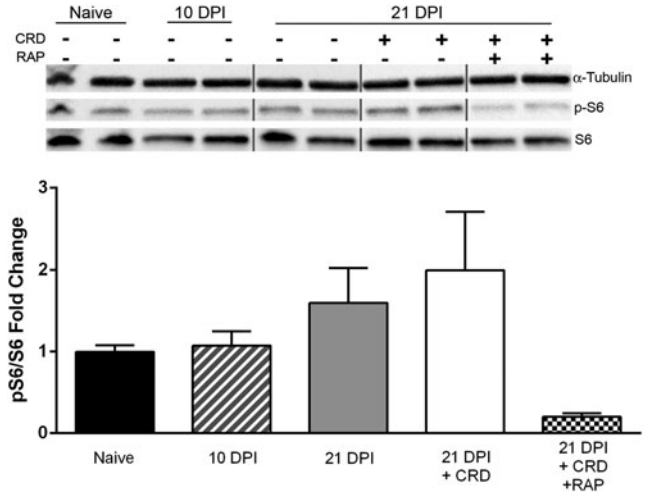

FIG. 1. Effects of rapamycin (RAP) treatment on mammalian target of rapamycin (mTOR) activity after spinal cord injury (SCI). Western blot analysis showed elevated mTOR activity after both SCI and colorectal distension (CRD) at 21 days post-injury (DPI), but prolonged treatment with RAP (3 mg/kg intraperitoneally, every other day) suppressed mTOR activity in the lumbosacral spinal cord. The ratio of phosphorylated-S6 ribosomal protein to total S6 is used as a downstream indicator of mTOR activity. As a loading control, α-tubulin was used, and values are expressed relative to naïve control values. Vertical grey lines separate lanes of groups not assessed (i.e., other days post-injury with no changes). Statistical analysis was not performed because of the low sample size ($n = 2$ per group). Symbols are means ± standard deviation.

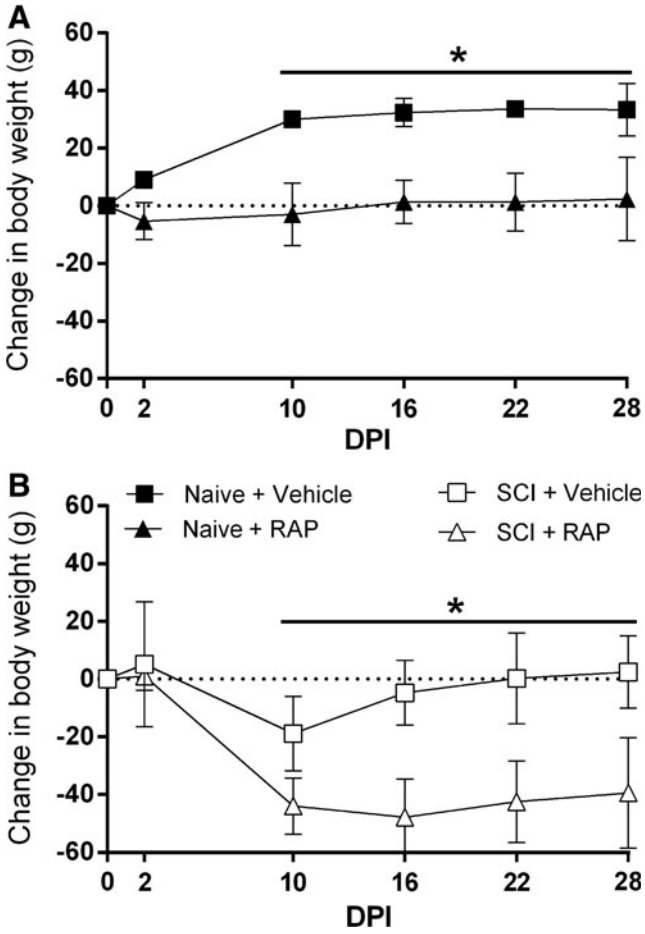

FIG. 2. Body weight dynamics after prolonged rapamycin (RAP) treatment and spinal cord injury (SCI). The RAP treatment prevented weight gain in both naïve and SCI rats. (**A**) The RAP prevented the normal increase in body weight over time in naïve, vehicle-treated rats. (**B**) After SCI, vehicle-treated rats started to regain weight by 16 days post-injury (DPI), whereas RAP-treated rats lost significantly more weight by 10 DPI and failed to approach pre-injury body weights. $n = 3$ naïve + vehicle; $n = 3$ naïve + RAP (3 mg/kg); $n = 7$ SCI + vehicle; $n = 7$ SCI + RAP (3 mg/kg). Symbols are means ± standard deviation. $^*p \leq 0.05$, vehicle vs. RAP treatment.

During each CRD trial, the balloon was inflated with 2 mL of air for 60 sec, followed by a 10-min rest interval. Using the Dataquest A.R.T. Acquisition software, ''event markers'' were placed at the beginning and end of each CRD trial trace to demarcate CRD-induced cardiovascular changes. Immediately after the second CRD trial at 28 DPI, a final session of prolonged, intermittent CRD was initiated to induce c-Fos expression as described.[17] Briefly, this procedure lasted 90 min with 30-sec inflation periods separated by 60-sec rest periods. With this paradigm, a total of 60 rounds of catheter inflation were performed. For all CRD trials, the balloon catheter was fully inflated with 2 mL of air within 5 sec.

For measurements of CRD-induced changes in blood pressure and HR, the raw pulsatile arterial pressure data were averaged every 2 sec and converted into MAP traces for analysis in the Dataquest A.R.T. Analysis software. The inter-beat interval was

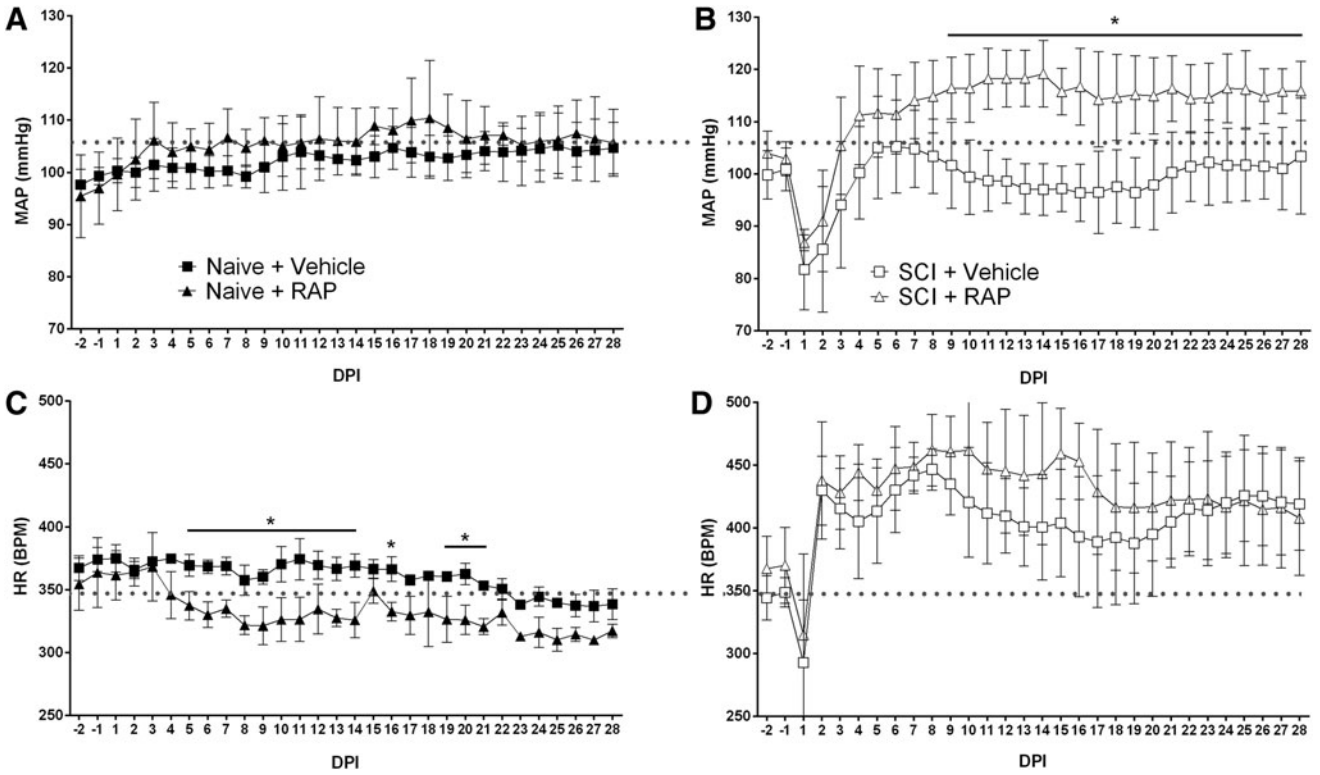

FIG. 3. Rapamycin (RAP) effects on cardiophysiology of naïve and spinal cord injured (SCI) rats. (**A**) Chronic RAP treatment did not alter daily mean arterial pressure (MAP) in naïve rats across days post-injury (DPI), but it caused significantly elevated MAP in rats with SCI (**B**) beginning at nine DPI to levels much higher than naïve controls (horizontal dotted lines). (**C**) In naïve rats, RAP significantly decreased heart rate (HR) across DPI, whereas highly elevated HR starting days after SCI was unaltered by RAP (**D**). $n = 3$ naïve + vehicle; $n = 3$ naïve + RAP (3 mg/kg); $n = 7$ SCI + vehicle; $n = 7$ SCI + RAP (3 mg/kg). Symbols are means ± standard deviation. $^*p \leq 0.05$ vehicle vs. RAP treatment. BPM, beats per min.

derived from the pulsatile arterial pressure waveform and converted to BPM to generate a separate heart rate (HR) trace. For each trial, the absolute MAP and HR values achieved during CRD stimulation were measured by averaging all data points within the 60-sec window of balloon inflation. In addition, pre-CRD baseline MAP and HR values were generated by averaging all data points within the 30-sec window immediately before the balloon inflation event marker, and CRD-induced changes in MAP and HR were then calculated as the difference between the respective 30-sec baselines and the values achieved during CRD. At each time-point

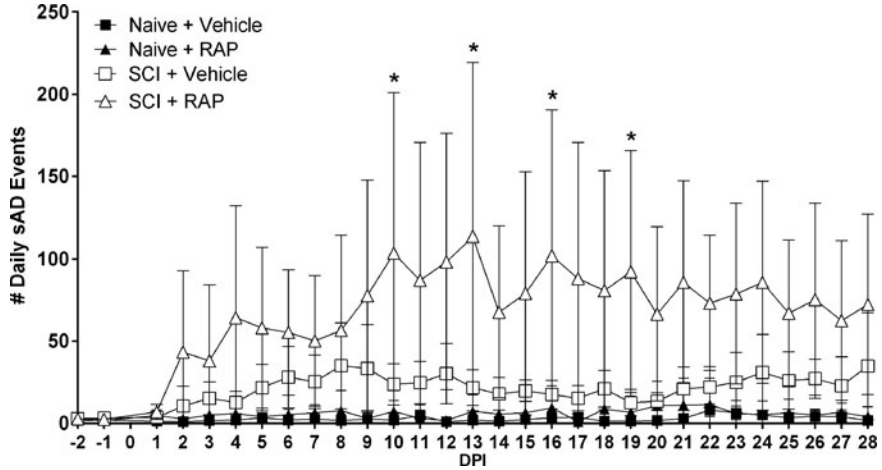

FIG. 4. Rapamycin (RAP) treatment effects on the daily frequency of spontaneously occurring AD (sAD) events. Compared with vehicle-treated naive rats, the vehicle-treated spinal cord injury (SCI) group had conspicuously more sAD events over all days post-injury (DPI). RAP significantly increased the frequency of sAD compared with vehicle-treated SCI rats, however. $n = 3$ naïve + vehicle; $n = 3$ naïve + RAP (3 mg/kg); $n = 7$ SCI + vehicle; $n = 7$ SCI + RAP (3 mg/kg). Symbols are means ± standard deviation. $^*p \leq 0.05$ vs. SCI + vehicle.

(14, 21, 28 DPI), the values of the two replicate CRD trials were averaged for each rat in the data analyses.

Western blot analysis

For the cohort of age and sex-matched Wistar rats ($n = 10$) used for Western blotting, the L6-S2 spinal cord segment was rapidly dissected and flash frozen in liquid nitrogen, after CO_2 euthanasia and decapitation. Samples were mechanically homogenized in ice-cold radioimmunoprecipitation assay (RIPA) buffer with 5 mm sodium fluoride and protease inhibitors (Cat# 11836153001, Sigma Aldrich, St. Louis, MO) added to preserve protein phosphorylation status and maintain total protein integrity; 1 mL of RIPA buffer was added per gram of tissue to manually grind samples in a dounce homogenizer before brief (3×10 sec) ultrasonic homogenization.

The Pierce BCA Protein Assay Kit (Cat# 23225, Thermo Fisher Scientific, Waltham, MA) was used to estimate the total protein concentration of each sample, and 20 μg of total protein from each spinal cord sample were suspended in Laemmli buffer under reducing conditions (5% β-mercaptoethanol) and then separated by sodium dodecyl sulfate polyacrylamide gel electrophoresis (SDS–PAGE) using 4-20% Criterion TGX pre-cast gels (Cat# 5671094, Bio-Rad, Hercules, CA). Separated proteins were transferred onto nitrocellulose membranes using the Trans-Blot Turbo Transfer System (Cat# 1704150, Bio-Rad, Hercules, CA). Nitrocellulose membranes were blocked with non-fat dry milk (5% in tris-buffered saline/Tween20 [TBST]) for 1 h at room temperature. Blocked membranes were then incubated at 4°C overnight in primary antibody diluted in blocking buffer. After primary incubation, membranes were washed for 3×20 min in TBST before incubating for 1 h at room temperature in secondary antibody diluted in blocking buffer. Excess secondary antibody was then removed by washing for 3×20 min in TBST.

Immunolabeled membranes were developed using enhanced chemiluminescence (Amersham ECL Advance Western Blotting Detection Kit, GE Healthcare, UK) and imaged with the ChemiDoc MP system (Bio-Rad). Quantification was then performed with ImageJ software (National Institutes of Health, Washington, DC) by plotting individual lanes and quantifying the area under the curve.[25,36] Antibodies were used according to manufacturer data sheets: pS6 (1:1,000; Cell Signaling Technology # 2215), S6 (1:1,000; Cell Signaling Technology # 5G10), α-tubulin (mouse monoclonal 1:10,000; Abcam #ab7291), horseradish peroxidase (HRP) conjugated goat-anti-rabbit (1:5000; Jackson Immunoresearch Cat# 111-035-144), HRP conjugated goat-anti-mouse (1:5000; Jackson Immunoresearch Cat#115035166). All lanes were normalized to their respective α-tubulin loading control, and fold-changes were expressed relative to naïve values.

Tissue fixation and processing

At 28 DPI, all rats undergoing cardiophysiological monitoring were euthanized within 10 min after the 90-min CRD protocol with an overdose of sodium pentobarbital (Fatal Plus, Vortex Pharmaceuticals, Dearborn, MI) before perfusion transcardially with 0.1 M PBS, pH 7.4, followed by 4% paraformaldehyde (PFA) in PBS.[16] A 3-cm segment of cord measured from the conus medullaris was dissected and the dura mater carefully removed before post-fixing in 4% PFA for 4 h and storing overnight in 0.1M PB at

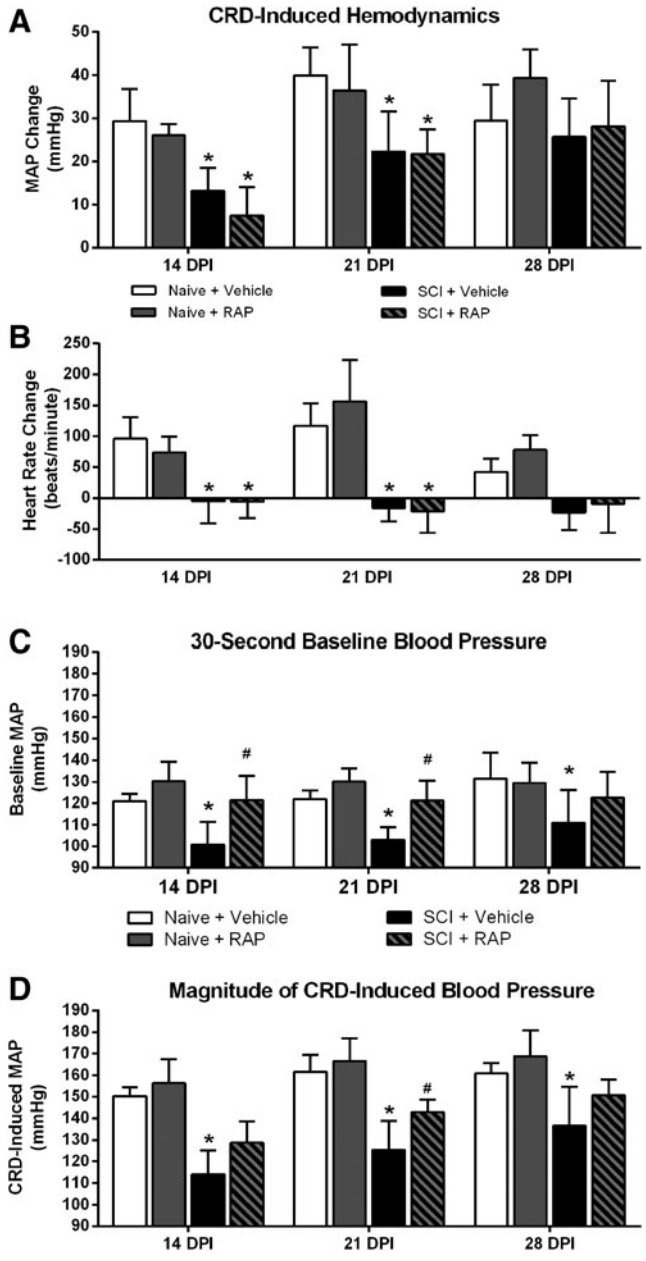

FIG. 5. Effects of prolonged rapamycin (RAP) treatment on mean arterial pressure (MAP) and heart rate (HR) during colorectal distension (CRD). (**A**) In naïve rats, RAP treatment did not affect the extent of CRD-induced MAP change relative to baseline at any time point. Spinal cord injury (SCI) alone significantly attenuated the extent of CRD-induced MAP changes at 14 and 21 days post-injury (DPI), but RAP treatment after SCI did not alter the extent of MAP response to CRD at any time point. (**B**) Naïve rats responded to CRD with tachycardia, whereas injured rats displayed bradycardia that is characteristic of AD. While the HR responses to CRD were diametrically opposite in injured compared with naïve rats at all DPI, RAP treatment did not alter the extent of CRD-induced HR changes in either naïve or SCI groups. (**C**) RAP treatment did not alter the baseline MAP in naïve rats at any time point. SCI significantly reduced the baseline MAP compared with the naïve + vehicle group at 14, 21, and 28 DPI, however. In SCI rats, RAP significantly increased the baseline-MAP to naïve levels compared with the SCI + vehicle group at 14 and 21 DPI. (**D**) The absolute MAP reached during CRD was lower in SCI rats at all time points. Whereas RAP treatment had no effects in naïve rats, it significantly increased the CRD-induced MAP in injured rats at 21 DPI. $n = 3$ naïve + vehicle; $n = 3$ naïve + RAP (3 mg/kg); $n = 7$ SCI + vehicle; $n = 7$ SCI + RAP (3 mg/kg). Symbols are means ± standard deviation. *$p < 0.05$ vs. naïve + vehicle; #$p < 0.05$ vs. SCI + vehicle.

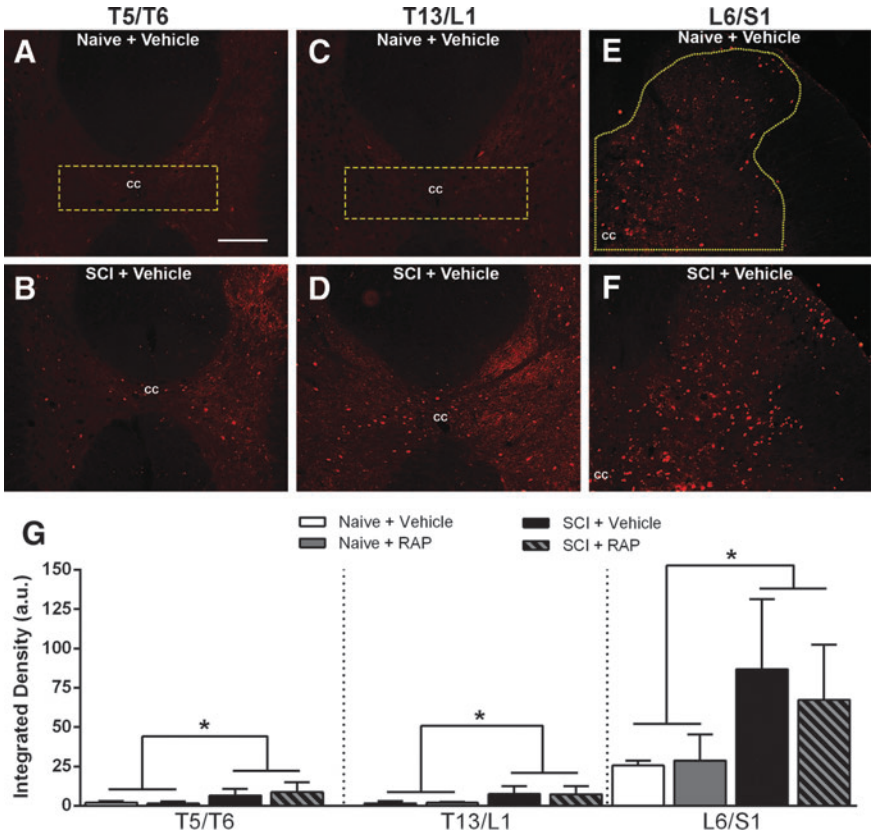

FIG. 6. Representative images of c-Fos immunostaining in cross sections from the T5/T6, T13/L1 and L6/S1 spinal segments of vehicle-treated naïve (**A,C,E**) and spinal cord injury (SCI) (**B,D,F**) rats after prolonged, intermittent colorectal distension (CRD). The regions of interest used for quantification are delineated by yellow dashed lines in A, C, E. The c-Fos immunoreactivity was increased after SCI + CRD compared with naïve + CRD throughout the dorsal gray commissure (DGC) in thoracic levels (A–D) and dorsal horn of lumbosacral segments (E,F). However, treatment with rapamycin (RAP) did not appear to alter immunoreactivity (**G**). cc = central canal. Bar = 200 μM, applies to all. (G) Densitometric analysis revealed that CRD led to significantly increased c-Fos immunoreactivity at all levels in the SCI groups compared with naïve, but there were no significant treatment effects within groups. When groups were collapsed according to injury status, there was a significant increase in c-Fos densities in the thoracic DGC and lumbosacral dorsal horn after SCI. $n = 3$ naïve + vehicle; $n = 3$ naïve + RAP (3 mg/kg); $n = 7$ SCI + vehicle; $n = 7$ SCI + RAP (3 mg/kg). Symbols are means ± standard deviation. * $p < 0.05$ naïve vs. SCI groups. Color image is available online at www.liebertpub.com/neu

4°C. Tissue was then cryopreserved with 20% sucrose in 0.1M PBS solution with 0.002% sodium azide at 4°C until all cords had sunk to the bottom of their container.

Spinal cords were embedded in a mixture of gum tragacanth (Sigma Aldrich, St. Louis, MO) and 20% sucrose in 0.1M PBS by evenly aligning 4–6 cords side by side within plastic cryomolds that were then snap frozen in −40°C acetone and stored at −80°C until sectioning on a cryostat (Microm Laborgerate, Walldorf, Germany). Frozen tissue blocks were sectioned in the transverse plane at a thickness of 20 μm, and every fifth section (100 μm spacing) was mounted onto one of three series of 10 slides (Superfrost, Fisher Scientific, Waltham, MA), consecutively (i.e., 1–10 thoracolumbar; 1a–10a lumbar; 1b–10b lumbosacral). Up to 15 consecutive rows of cryosections from each block were placed onto each of 10 slides in all three series. In this manner, 0.5 mm separation is represented by two slides separated by five within the series of 10 processed for histological analysis (i.e., slides 1 and 6, 1a and 6a, 1b and 6b). All slides were stored at −20°C until used for histological staining.

Immunohistochemistry and microscopy

Mounted slides were removed from the freezer to thaw at room temperature for 30 min before a series of 3 × 10-min washes in 0.1M PBS with gentle agitation to rehydrate tissue and remove excess embedding media. They were then pre-incubated in blocking buffer consisting of 0.1M PBS containing 0.3% Triton-X and 5% normal goat serum. Tissue was then incubated with primary antibody overnight at 4°C in blocking buffer containing rabbit-anti-CGRP 35.3 (μg/mL; Sigma #C8198) and mouse-anti-c-Fos (2 μg/mL; Encor Biotechnology #MCA-2H2). After primary antibody incubation, slides were washed 3 × 10 min in 0.1M PBS. Next, slides were incubated overnight at 4°C in blocking buffer containing goat-anti-rabbit conjugated to Alexa-488 (4 μg/mL; Life Technologies #A11008) or biotinylated goat-anti-mouse (7.5 μg/mL; Vector #BA9200).

The following day, slides were washed 3 × 10 min in 0.1M PBS, and c-Fos sections were shielded from light and incubated for another 4 h at room temperature with Texas Red conjugated streptavidin (3.33 μg/mL, Vector #SA-5006) in 0.1M PBS. All slides were washed 3 × 10 min in 0.1M PBS before cover-slipping with Vectashield mounting media (Vector #H-1000) containing 5 μM Hoechts dye (#H3570, Thermo Fisher) to stain nuclear deoxyribonucleic acid. All images acquired for both CGRP and c-Fos quantification were captured using an Olympus BX51 microscope paired with an Olympus Magnafire digital camera (Melville, NY). Image exposure times were kept constant to help maintain a consistent level of background staining.

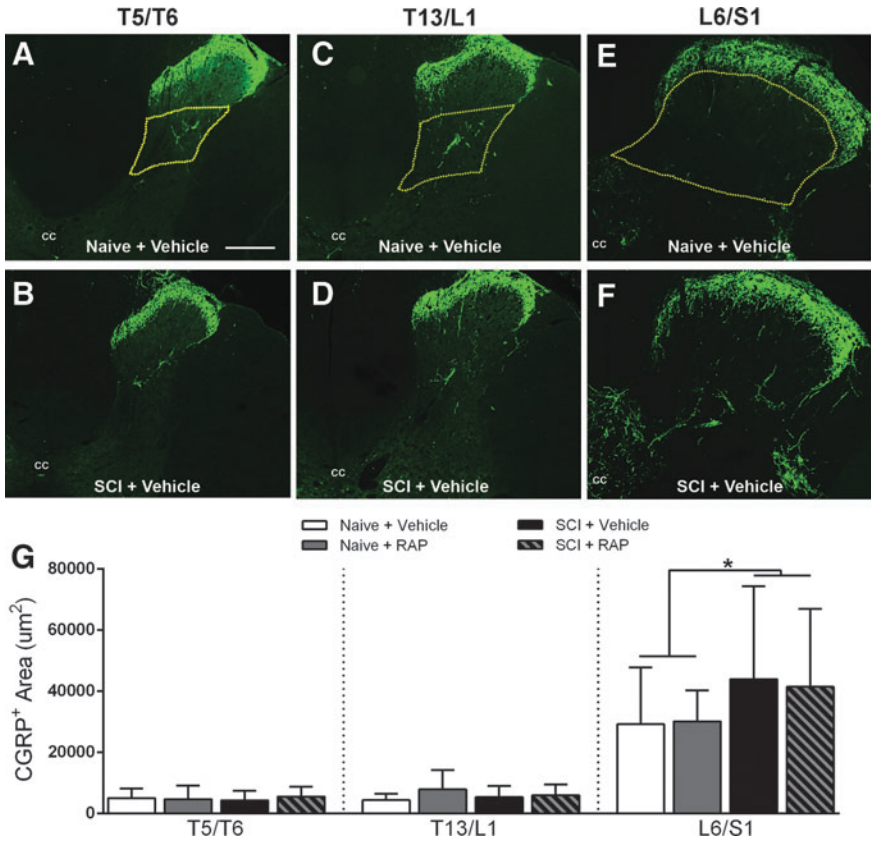

FIG. 7. Representative images of calcitonin gene related peptide (CGRP) immunostaining in cross sections from the T5/T6, T13/L1 and L6/S1 spinal segments of naïve (**A,C,E**) and injured (**B,D,F**) spinal cords four weeks after SCI. There were no apparent injury or rapamycin (RAP) treatment effects in thoracic levels (A–D), whereas increased densities of $CGRP^+$ fibers in deep dorsal horn laminae of L6/S1 segments were seen after SCI (F). The regions of interest (ROI) used for quantification are delineated by yellow dashed lines. Bar = 200 μM, applies to all. (**G**) Densitometric analysis of CGRP+ c-fibers in lumbosacral dorsal horn revealed no significant RAP effects in naïve or injured groups, but when groups were collapsed according to injury status, there was a significant increased $CGRP^+$ fiber densities in the L6/S1 segment after SCI. cc = central canal. $n = 3$ naïve + vehicle; $n = 3$ naïve + RAP (3 mg/kg); $n = 7$ SCI + vehicle; $n = 7$ SCI + RAP (3 mg/kg). Symbols are means ± standard deviation. * $p < 0.05$ naïve vs. SCI groups. Color image is available online at www.liebertpub.com/neu

Densitometric analyses

For both c-Fos and CGRP densitometry analyses in the thoracic and lumbosacral cord, five serial coronal sections (1 mm spacing) centered on each of the three levels evaluated (T5/T6, T13/L1, and L6/S1 segments) were used for each rat. For c-Fos quantification, densitometry was performed using ImageJ software (National Institutes of Health, Bethesda, MD). All 24-bit red, green, blue (RGB) photomicrographs were converted into eight-bit black and white images, and the regions of interest (ROI) included the entire right dorsal horn for the L6/S1 level or the dorsal gray commissure for T5/T6 and T13/L1 levels (see Fig. 6). Thresholds for each c-Fos ROI were identified manually by a single experimenter based on the lowest pixel value above which c-Fos+ nuclei were included, and final values were expressed in arbitrary units.

For CGRP quantification, densitometry of digitized 24-bit RGB photographs from the thoracic and lumbosacral levels was performed using Bioquant image analysis software (Nova Prime; V6.70.10; Bioquant Image Analysis Corp., Nashville, TN) with the ROI demarcated by laminae III-V in the dorsal gray matter for the L6/S1 level or laminae IV for the T5/T6 and T13/L1 levels to account for differential cytoarchitecture (see Fig. 7). Thresholds for each CGRP ROI were chosen by a single experimenter based on the pixel values above which the faintest $CGRP^+$ fibers were included. The CGRP measurements were calibrated inside of Bioquant software to express results in μm^2.

Statistical analyses

All statistical analyses were conducted using Prism 6.0 software (Graphpad Software, La Jolla, CA), with alpha set at 0.05. For measurements over time of body weight, daily MAP and HR, CRD-induced changes, and daily spontaneous AD data sets, two-way repeated measures analysis of variance (ANOVA) were conducted followed by Sidak *post hoc* when appropriate. The Geisser-Greenhouse correction factor was used for all repeated measures ANOVAs to adjust for deviations from the compound symmetry assumption within our data. For analysis of c-Fos and CGRP histological data, ANOVA and Sidak *post hoc* were used, followed by unpaired *t* tests on collapsed data when warranted.

Results

We recorded a 30% attrition rate in the SCI + RAP group undergoing telemetric monitoring, with 3/10 rats in this group dying of unknown causes within three weeks post-injury and the start of treatment. These animals were accordingly excluded from all

analyses, resulting in a final group size of $n=7$. Notably, no unexpected attrition occurred in the naïve or SCI + vehicle groups, or in any of the groups used for Western blotting.

RAP reduces mTOR activity in the injured spinal cord

We examined mTOR activity in the lumbosacral segments after SCI and noxious CRD using Western blot assessments of phosphorylated S6 ribosomal protein (pS6), a widely used downstream marker of mTOR activity.[25,37,38] Relative to naïve spinal cords, those from 10 and 21 DPI showed heightened S6 phosphorylation in the lumbosacral spinal cord (Fig. 1). The CRD at 21 DPI further augmented mTOR activity by approximately two-fold; however, prolonged RAP administration prevented such increases, notably reducing pS6 levels below even naïve values.

RAP treatment impairs normal weight gain and exacerbates weight loss after SCI

Body weight data were compared between vehicle control and RAP-treated groups before and during prolonged RAP administration. In naïve rats, there were significant effects of time ($p<0.0001$), treatment ($p=0.0079$), and interaction ($p<0.0001$) on body weight (Fig. 2A). Naïve + vehicle rats gained approximately 30 g of body weight by 10 DPI, whereas naïve + RAP rats maintained stable body weights for the duration of the study and weighed significantly less than naïve + vehicle rats beginning at 10 DPI ($p<0.0001$). In injured rats, there were also significant effects of time ($p<0.0001$), treatment ($p=0.0002$), and interaction ($p<0.0001$) on body weight (Fig. 2B). The SCI + vehicle rats lost approximately 15 g of body weight over the first 10 DPI and subsequently returned to their pre-injury weight by 16 DPI. Conversely, SCI + RAP rats lost approximately 40 g in the first 10 DPI and failed to return to pre-injury weights by the end of the study (Fig. 2B). Similar to the naïve groups, a significant treatment effect to reduce weight was apparent by 10 DPI, which remained significantly lower for the remainder of the study ($p<0.05$).

RAP alters daily hemodynamic measures before and after SCI

We investigated the effect of prolonged RAP treatment on the average daily MAP and HR in naïve and injured rats over four weeks. In naïve rats, there was a significant effect of time on daily MAP (Fig. 3A; $p<0.0001$), but no differences in the average daily MAP between naïve groups across time ($p=0.4758$). In rats with SCI, there were significant effects of time post-injury (Fig. 3B; $p<0.0001$) and treatment ($p=0.0003$) on daily MAP, along with a significant interaction between time and treatment ($p<0.0001$). When compared with their respective pre-injury values, the average daily MAP in both vehicle- and RAP-treated SCI groups declined significantly ($p<0.001$) for two days post-injury before returning to pre-injury values (Fig. 3B). Rapamycin significantly elevated daily MAP above vehicle controls ($p<0.05$) beginning at nine DPI and lasting through the remainder of the study period, notably being maintained well above pre-injury control values (Fig. 3B).

In naïve rats, there were significant effects on daily HR based on time post-injury ($p<0.0001$) and treatment ($p=0.0133$), as well as a significant interaction ($p=0.0008$) (Fig. 3C). Specifically, daily HR was significantly lower in naïve rats with RAP treatment versus naïve + vehicle controls between five and 21 DPI ($p<0.05$). Despite a trend for increased daily HR in SCI + RAP rats during weeks two and three post-injury, however, there was no significant treatment effect on HR ($p=2.066$). In sum, and paradoxically, RAP treatment in naïve rats did not alter MAP but significantly lowered HR, whereas after SCI it significantly increased daily MAP accompanied by only moderate HR increases.

RAP increases the frequency of spontaneous AD

We assessed the effects of RAP treatment on the daily frequency of spontaneously occurring AD (sAD) in freely moving naive and SCI rats using our sAD event detection algorithm applied to MAP and HR data corresponding to each day pre- and post-injury (Fig. 4). While there were negligible sAD events detected in the naïve groups across all time points, there were significant effects on the frequency of sAD events based on time post-injury ($p<0.0001$) and treatment ($p<0.0001$), along with a significant interaction ($p<0.0001$). Notably, the RAP-treated SCI group showed significantly higher frequencies of daily sAD compared with the SCI + vehicle group, such that by 16 DPI, a time by which AD becomes fulminant in T4Tx rats, the SCI + RAP group had $\sim$100 AD events/day compared with $\sim$20 events/day in the SCI + vehicle group.

RAP increases baseline and absolute MAP but not extent of CRD-induced AD

We first examined the extent of MAP increase during CRD in relation to 30-sec baselines, as is reported typically (Fig. 5A), and found significant effects of time ($p<0.0001$) and injury ($p=0.0037$), along with an interaction of time and injury ($p=0.0292$). When compared with naïve + vehicle, SCI + vehicle rats had significantly reduced MAP increases during CRD at 14 and 21 DPI ($p<0.05$). In both naïve and injured groups, however, RAP did not alter the extent of such MAP increases during CRD compared with respective 30-sec baselines (Fig. 5A).

In both naïve and injured groups, there was an overall effect of time post-injury on HR changes during CRD ($p=0.0052$), but no significant treatment effects ($p>0.05$; Fig. 5B). Notably, irrespective of treatment, naïve rats responded to CRD with pronounced tachycardia, whereas injured rats showed bradycardia that is characteristic of AD. Both SCI groups had significant drops in HR during CRD compared with the naïve groups at 14 and 21 DPI ($p<0.005$), with only a trend for lower HR in the injured groups at 28 DPI ($p=0.056$).

While this would appear to indicate no effect of RAP on CRD-induced AD, we next compared baseline MAP values of naïve and injured rats at rest during the 30 sec preceding CRD (Fig. 5C). There was an overall significant treatment effect on the pre-CRD baseline MAP values ($p=0.0008$), but no effect of time post-injury ($p=0.1291$). The baseline MAP was significantly ($p<0.05$) lower in the SCI + vehicle groups compared with the naïve + vehicle groups at 14, 21, and 28 DPI. Critically, however, the SCI + RAP group had significantly higher pre-CRD baseline MAP compared with the SCI + vehicle group at 14 and 21 DPI ($p<0.05$), effectively normalizing pre-CRD baselines to naïve control levels. Notably, the significant increase in pre-CRD MAP in SCI + RAP versus SCI + vehicle rats is consistent with the significantly increased daily 24-h MAP in RAP- versus vehicle-treated SCI rats.

Accordingly, there were significant effects of RAP on the absolute magnitude of MAP reached during CRD based on time ($p<0.0001$) and treatment ($p<0.0001$), with no interaction ($p=0.2455$) (Fig. 5D). The SCI alone resulted in significantly lower absolute MAP induced by CRD compared with both naïve groups at 14, 21, and 28 DPI ($p<0.05$). While RAP treatment did not alter the absolute MAP reached during CRD in naïve rats, however, the

SCI + RAP group had a significantly higher MAP during CRD ($\sim$143 mm Hg) compared with SCI + vehicle rats ($\sim$125 mm Hg) at 21 DPI ($p < 0.05$). While the absolute MAP reached during CRD did not change over time in the naïve groups, there were significant increases over time in both SCI groups. In the SCI + vehicle group, the absolute CRD-induced MAP increased significantly from 14 to 21 DPI ($p < 0.005$), 14 to 28 DPI ($p < 0.0001$), and 21 to 28 DPI ($p < 0.005$). Similarly, the absolute CRD-induced MAP in the SCI + RAP group increased from both 14 to 21 DPI ($p < 0.0005$) and 14 to 28 DPI ($p < 0.0001$). While not statistically significant, there was a trend for the CRD-induced MAP to increase from 21 to 28 DPI in the SCI + RAP group ($p = 0.055$).

RAP does not alter density of c-Fos or CGRP immunolabeling

After prolonged, intermittent CRD, we measured the density of c-Fos immunolabeling in the dorsal gray commissure (DGC) at the T5/T6 and T13/L1 spinal cord levels (Fig. 6A–D), which contain propriospinal interneurons that relay noxious pelvic sensory information toward thoracic SPNs,[17,39,40] as well as the dorsal horn of the L6/S1 spinal cord (Fig. 6E, F), which receives colorectal afferents. The c-Fos is an immediate early gene widely used as a marker of neuronal activation in response to electrical or sensory stimulation.[41] In naïve rats with intact descending modulatory pathways, we observed sparsely distributed c-Fos$^+$ nuclei throughout the thoracic DGC (Fig. 6A, C) and lumbosacral dorsal horn gray matter (Fig. 6E) after prolonged CRD, which qualitatively increased in density after SCI (Fig. 6B, D, F). An ANOVA revealed that the density of c-Fos was unaltered by RAP treatment in the T5/T6, T13/L1 or L6/S1 spinal levels (Fig. 6G). When data were collapsed into two groups based on injury status (naïve or injured), *t* tests showed that rats with SCI had significantly increased c-Fos density at all three spinal levels when compared with naïve rats ($p < 0.05$).

We also evaluated the density of CGRP$^+$ fiber labeling in the thoracic and lumbosacral dorsal horn to determine whether RAP altered sprouting of unmyelinated primary afferents conveying noxious stimuli into the spinal cord. In naïve rats, thoracic CGRP immunolabeling was restricted primarily to the substantia gelatinosa and lamina IV (Fig. 7A–D). In the lumbosacral cord, CGRP$^+$ labeling was located typically in the substantia gelatinosa, dorsal gray commissure, and around the sacral parasympathetic nucleus (Fig. 7E, F). After injury, there were qualitative increases in fiber labeling throughout the L6/S1 segments (Fig. 7E) that were not apparent in the thoracic segments (Fig. 7B, D). An ANOVA across all groups at each level showed no significant treatment effects in naïve or injured rats. When data were collapsed into two groups based on injury status (naïve or injured), the lumbosacral segment had significantly more CGRP$^+$ fiber density after SCI compared with naïve groups ($p = 0.0081$; Fig. 7G), but no injury effects were observed at either thoracic level ($p > 0.05$; Fig. 7B, D).

Discussion

While the mTOR pathway has been targeted as a modulator of post-traumatic plasticity as well as pain development, no studies have examined the effects of mTOR inhibition on cardiovascular and autonomic dysfunction after SCI. We report that prolonged every-other-day RAP treatment leads to significantly elevated resting blood pressure, increased blood pressure volatility, and exacerbated weight loss after experimental SCI. While the extent of MAP increases relative to 30-sec baseline during noxious CRD was unaltered by treatment, the baseline MAP preceding CRD was significantly higher at two and three weeks post-injury, and the absolute magnitude of CRD-induced MAP was significantly higher three weeks post-injury in RAP-treated rats.

Because there were no treatment effects on the sprouting of c-fiber afferents or c-Fos expression in interneurons, these confounding cardiovascular effects of RAP after SCI appear to result from other unidentified central and/or peripheral mechanisms. Moreover, these results indicate that, unlike hippocampal pathway sprouting after traumatic brain injury,[25] intraspinal plasticity of ascending nociceptive pathways contributing to AD after SCI is not dependent on mTOR signaling. Although we did not investigate the effects of a single administration of RAP at a clinically relevant time point, our data show that the adverse cardiovascular effects started soon after the first drug administration. Notably, there were trends for increased daily MAP and sAD in the SCI + RAP group as early as two to three days post-injury, and given our every-other-day treatment paradigm, this suggests that a single dosage immediately after SCI can elicit adverse cardiovascular effects. This would again support a mechanism that is not dependent on inhibiting intraspinal plasticity, but rather altering resistance of peripheral vasculature.

Alternatively, the marked increase in sAD events in rats with SCI treated with RAP may stem from a lowering of the threshold needed for afferent stimulation to trigger an AD event. For instance, long-term treatment of patients with cancer and organ transplant recipients with mTOR inhibitors, including RAP and closely associated derivatives such as everolimus, increases the incidence of pain development.[42–45] Moreover, RAP also induces significant tactile hypersensitivity in both naïve and spinal nerve ligated rodents.[46] Chronic mTOR inhibition can result in overactivation of the extracellular signal-regulated kinase (ERK) signaling pathway in sensory neurons, purportedly through disinhibition of the insulin receptor substrate (IRS), which functions upstream of ERK.[46] Notably, ERK activation is involved in the regulation of nociceptive neurons,[47,48] suggesting that prolonged RAP treatment may increase nociceptor sensitivity by inducing feedback stimulation of the ERK pathway. Such feedback stimulation may lower the threshold of afferent stimulation needed to trigger AD, thus increasing the frequency of sAD in RAP-treated rats with SCI independent of structural plasticity associated with the development of AD.[16,17]

Conversely, a number of studies suggest that RAP treatment can prevent the development of pain after SCI. A single intraperitoneal (IP) injection of RAP given 4 h after T10 contusion SCI in mice suppresses microglial activation and neuropathic pain weeks after injury.[49] Similarly, pharmacological inhibition of mTOR has been associated with reduced CGRP protein expression in the spinal cord after traumatic SCI in rats.[29] A single intrathecal infusion of RAP (10 μg) or LY294002 (10 μM), an inhibitor of the upstream PI3K, administered after SCI attenuates injury-induced increases in CGRP protein expression in the dorsal horn.[29] This finding was correlated with reduced indices of neuropathic pain after SCI, suggesting that acute and local RAP administration attenuates the development of neuropathic pain after injury by disrupting the production or release of CGRP in the spinal cord dorsal horn.

Importantly, our findings instead show that prolonged IP RAP administration does not change CGRP$^+$ fiber density in the lumbosacral cord and suggests that it may possibly increase nociceptive neurotransmission as indicated by a significantly higher frequency of spontaneous AD events. These opposing effects of RAP on CGRP expression may be because of the difference in route and length of RAP administration, possibly reflecting an unintended

feedback stimulation of ERK[46] or other nociceptive signaling pathways in our chronic treatment paradigm. In support of this notion, *in vitro* and *in vivo* studies suggest that prolonged versus acute RAP administration has differential effects on metabolism and cellular signaling.[50,51]

Regarding the significantly increased basal MAP with RAP treatment, both resting and orthostatic hypotension are clinically vital issues, particularly for individuals with severe cervical or high-thoracic SCI.[52,53] Therefore, treatments capable of increasing resting MAP may be therapeutically valuable for the SCI population. Similar to previous reports,[31,54–56] we observed that SCI resulted in a decreased daily MAP lasting for several days that gradually returned to near-normal levels within three weeks post-injury in vehicle-treated rats. Conversely, the acute decrease in daily MAP after SCI was followed by significant elevations in daily MAP in RAP-treated rats within approximately one week after injury. In fact, the daily MAP levels reached were higher than pre-injury levels or even controls, indicating that prolonged RAP treatment may alleviate symptoms associated with hypotension, such as weakness and dizziness. We did not, however, examine daily systolic blood pressure to assess whether prolonged RAP treatment after complete SCI significantly increases resting systolic blood pressure to potentially harmful levels.

Although RAP treatment did not significantly increase daily HR after injury, it is feasible that the slightly higher HR in RAP animals contributed to the significant increase in daily MAP. One possible mechanism for such a tachycardia-mediated increase in MAP is through increasing cardiac output (CO), which can be described as the product of stroke volume (SV) and heart rate ($CO = SV \times HR$). In relation to MAP, which is broadly determined as the function of CO and total peripheral resistance ($MAP = CO \times TPR$), the enhancement in CO could increase MAP in the absence of modified peripheral resistance.[57] In our injury model, supraspinal sympathetic control of the heart remains intact because the heart is innervated by T1-T3 SPNs.[58] Moreover, evidence suggests that mTOR activity in the hypothalamus is involved in the regulation of blood pressure and sympathetic nerve activity,[37] and hypothalamic mTOR controls feeding behavior,[59] which could partially explain both the decreased body weight and increased daily MAP in SCI + RAP animals in our study.

We observed that RAP significantly exacerbated injury-induced weight loss and prevented rats from returning to their pre-injury weight. A significant decrease in body weight has been observed in naïve male Wistar rats treated daily for three weeks with sirolimus (IP 2 mg/kg), which is a clinical formulation of injectable RAP.[60] This was associated with significantly decreased food intake, suggesting that the effects of RAP on body weight are mediated through changes in appetite and energy intake. Single IP injections of RAP are sufficient to reduce daily food intake and weight gain for several days in naïve rats.[61] Notably, the effects of such injections on body weight persisted for at least 10 weeks, indicating that a single dosage of RAP can cause a permanent shift in body weight set point. Hypothalamic mTOR activity is thought to play a role in the control of feeding, as intracerebroventricular delivery of RAP decreases food intake in rats treated with the appetite-stimulating hormone, ghrelin.[59] Although we did not monitor food intake in our study, it is possible that the effects of RAP we observed in both naïve and SCI rats are, at least in part, from changes in feeding behavior because RAP can cross the blood–brain barrier.[62]

Critically, the significant and sustained reductions in body weight with RAP treatment in injured rats, in conjunction with elevated resting MAP and blood pressure volatility, likely put this group at a higher risk for secondary complications. Reductions in body weight result in significantly reduced cardiac ventricular size and stroke volume in rats,[63] suggesting that CO would be reduced in SCI + RAP rats. Because these rats, however, had elevated daily MAP, which is the product of CO and TPR, this implies that RAP treatment after injury increases TPR. Notably, such an increase in TPR after complete SCI would likely increase the total afterload against which the left ventricle would need to pump (i.e., aortic pressure),[64] placing additional stress on an already compromised cardiovascular system.

While the change in MAP relative to the baseline calculated from the 30 sec before CRD was not altered by RAP treatment, the absolute magnitude of blood pressure elevation during CRD was significantly higher in SCI + RAP rats three weeks after injury. This rise in absolute CRD-induced MAP indicates that RAP treatment has cardiophysiological consequences that could potentially increase the secondary consequences of AD, including stroke or hypertensive encephalopathy.[10,12] There are other reports of hypertension induced by RAP in otherwise healthy rats. Daily oral administration of 1 mg/kg RAP to male Wistar rats for seven weeks significantly elevated systolic (115 mm Hg to 148 mm Hg) and diastolic (99 mm Hg to 126 mm Hg) blood pressure compared with vehicle-treated rats.[65] This RAP-induced hypertension was associated with significantly elevated levels of plasma serotonin (5-hydroxytryptamine; 5-HT). Because vasoactive plasma 5-HT can cause vasoconstriction in multiple vascular beds,[66] such RAP-induced increases in plasma 5-HT may manifest as increased peripheral vascular resistance and resting blood pressure.

While we did not measure plasma 5-HT, it is feasible that the increased resting MAP observed in our study after prolonged RAP treatment was because of such alterations in plasma 5-HT. Given our peripheral (IP) route of drug administration, we are unable to delineate whether the RAP-induced hypertension seen in our SCI model was because of central or peripheral sites of action.

Other studies have investigated RAP as a neuroprotective agent after contusion SCI. A single 1 mg/kg (IP) dose of RAP administered 4 h after SCI in mice increases tissue sparing and functional recovery correlated with augmented cell autophagy.[67] Injections of 1 mg/kg (IP) of RAP daily for three days starting 4 h after SCI in rats also promotes neuronal survival by attenuating inflammatory responses.[34] A dosage of 6 mg/kg RAP (IP, every other day) administered for three weeks post-injury in rats normalizes increased mTOR activity after complete T10 transection in combination with passive exercise.[32] Whether the adverse cardiovascular effects of RAP we noted occur in the more clinically relevant contusion SCI model remains uncertain, although rodent contusion models of AD exist to test this.[68]

Conclusion

We sought to determine whether inhibiting mTOR activity with RAP could mitigate the development of AD by preventing injury-induced intraspinal plasticity. We found, instead, that RAP evoked significant physiological alterations in rats with complete high-thoracic SCI, including exacerbated body weight loss, increased resting blood pressure, increased spontaneous AD events, and increased magnitude of CRD-induced AD. Because inhibition of mTOR activity with RAP did not correlate with altered injury-induced sprouting of nociceptive afferents or activation of propriospinal neurons after noxious CRD, this indicates that mTOR does not act as a critical mediator of maladaptive plasticity thought to underlie AD. More broadly, the adverse cardiovascular effects are because of other unidentified central and/or peripheral

mechanisms that could arise from actions of RAP on dorsal root ganglia, peripheral sympathetic ganglia, or cardiovascular mechanisms involved in the modulation of peripheral vascular resistance. Critically, because cardiovascular complications after SCI are among the top health concerns clinically, studies investigating RAP as a neuroprotective therapy for SCI must take precaution in interpreting any outcome measures without considering unmonitored risks to already compromised cardiovascular and autonomic functions.

Acknowledgments

Special thanks to Dr. Richard Kryscio (University of Kentucky) for expert assistance in statistical analysis and Jensen Goh for assistance with immunohistochemistry procedures. This study was supported by 5T32 NS077889 (KCE), Craig H. Neilsen Foundation (AGR), SCoBIRC Chair Endowment (AGR), National Institutes of Health/National Institute of Neurological Disorders and Stroke P30 NS051220.

Author Disclosure Statement

No competing financial interests exist.

References

1. Devivo, M.J. (2012). Epidemiology of traumatic spinal cord injury: trends and future implications. Spinal Cord 50, 365–372.
2. Greenway, C.V. and Lister, G.E. (1974). Capacitance effects and blood reservoir function in the splanchnic vascular bed during non-hypotensive haemorrhage and blood volume expansion in anaesthetized cats. J. Physiol. 237, 279–294.
3. Rowell, L.B. (1990). Importance of scintigraphic measurements of human splanchnic blood volume. J. Nucl. Med. 31, 160–162.
4. Snow, J.C., Sideropoulos, H.P., Kripke, B.J., Freed, M.M., Shah, N.K., and Schlesinger, R.M. (1978). Autonomic hyperreflexia during cystoscopy in patients with high spinal cord injuries. Paraplegia 15, 327–332.
5. Lindan, R., Joiner, E., Freehafer, A., and Hazel, C. (1980). Incidence and clinical features of autonomic dysreflexia in patients with spinal cord injury. Spinal Cord 18, 285–292.
6. Marsh, D.R. and Weaver, L.C. (2004). Autonomic dysreflexia, induced by noxious or innocuous stimulation, does not depend on changes in dorsal horn substance p. J. Neurotrauma 21, 817–828.
7. Karlsson, A.K. (1999). Autonomic dysreflexia. Spinal Cord 37, 383–391.
8. Eltorai, I., Kim, R., Vulpe, M., Kasravi, H., and Ho, W. (1992). Fatal cerebral hemorrhage due to autonomic dysreflexia in a tetraplegic patient: case report and review. Paraplegia 30, 355–360.
9. Colachis, S.C., 3rd and Clinchot, D.M. (1997). Autonomic hyperreflexia associated with recurrent cardiac arrest: case report. Spinal Cord 35, 256–257.
10. Valles, M., Benito, J., Portell, E., and Vidal, J. (2005). Cerebral hemorrhage due to autonomic dysreflexia in a spinal cord injury patient. Spinal Cord 43, 738–740.
11. Jain, A., Ghai, B., Jain, K., Makkar, J.K., Mangal, K., and Sampley, S. (2013). Severe autonomic dysreflexia induced cardiac arrest under isoflurane anesthesia in a patient with lower thoracic spine injury. J. Anaesthesiol. Clin. Pharmacol. 29, 241–243.
12. Bjelakovic, B., Dimitrijevic, L., Lukic, S., and Golubovic, E. (2014). Hypertensive encephalopathy as a late complication of autonomic dysreflexia in a 12-year-old boy with a previous spinal cord injury. Eur. J. Pediatr. 173, 1683–1684.
13. Fausel, R.A. and Paski, S.C. (2014). Autonomic dysreflexia resulting in seizure after colonoscopy in a patient with spinal cord injury. ACG Case Rep. J. 1, 187–188.
14. Krassioukov, A.V., Johns, D.G., and Schramm, L.P. (2002). Sensitivity of sympathetically correlated spinal interneurons, renal sympathetic nerve activity, and arterial pressure to somatic and visceral stimuli after chronic spinal injury. J. Neurotrauma 19, 1521–1529.
15. Krenz, N.R., Meakin, S.O., Krassioukov, A.V., and Weaver, L.C. (1999). Neutralizing intraspinal nerve growth factor blocks autonomic dysreflexia caused by spinal cord injury. J. Neurosci. 19, 7405–7414.
16. Cameron, A.A., Smith, G.M., Randall, D.C., Brown, D.R., and Rabchevsky, A.G. (2006). Genetic manipulation of intraspinal plasticity after spinal cord injury alters the severity of autonomic dysreflexia. J. Neurosci. 26, 2923–2932.
17. Hou, S., Duale, H., Cameron, A.A., Abshire, S.M., Lyttle, T.S. and Rabchevsky, A.G. (2008). Plasticity of lumbosacral propriospinal neurons is associated with the development of autonomic dysreflexia after thoracic spinal cord transection. J. Comp. Neurol. 509, 382–399.
18. Brown, A., Ricci, M.J., and Weaver, L.C. (2004). NGF message and protein distribution in the injured rat spinal cord. Exp. Neurol. 188, 115–127.
19. Sandsmark, D.K., Pelletier, C., Weber, J.D., and Gutmann, D.H. (2007). Mammalian target of rapamycin: master regulator of cell growth in the nervous system. Histol, Histopathol, 22, 895–903.
20. Laplante, M. and Sabatini, D.M. (2012). mTOR signaling in growth control and disease. Cell 149, 274–293.
21. Dibble, C.C. and Manning, B.D. (2013). Signal integration by mTORC1 coordinates nutrient input with biosynthetic output. Nat. Cell Biol. 15, 555–564.
22. Sun, F., Park, K.K., Belin, S., Wang, D., Lu, T., Chen, G., Zhang, K., Yeung, C., Feng, G., Yankner, B.A., and He, Z. (2011). Sustained axon regeneration induced by co-deletion of PTEN and SOCS3. Nature 480, 372–375.
23. Liu, K., Lu, Y., Lee, J.K., Samara, R., Willenberg, R., Sears-Kraxberger, I., Tedeschi, A., Park, K.K., Jin, D., Cai, B., Xu, B., Connolly, L., Steward, O., Zheng, B., and He, Z. (2010). PTEN deletion enhances the regenerative ability of adult corticospinal neurons. Nat. Neurosci. 13, 1075–1081.
24. Jin, D., Liu, Y., Sun, F., Wang, X., Liu, X., and He, Z. (2015). Restoration of skilled locomotion by sprouting corticospinal axons induced by co-deletion of PTEN and SOCS3. Nat. Commun. 6, 8074.
25. Guo, D., Zeng, L., Brody, D.L., and Wong, M. (2013). Rapamycin attenuates the development of posttraumatic epilepsy in a mouse model of traumatic brain injury. PLoS One 8, e64078.
26. Schmelzle, T. and Hall, M.N. (2000). TOR, a central controller of cell growth. Cell 103, 253–262.
27. Asante, C.O., Wallace, V.C., and Dickenson, A.H. (2009). Formalin-induced behavioural hypersensitivity and neuronal hyperexcitability are mediated by rapid protein synthesis at the spinal level. Mol. Pain 5, 27.
28. Liang, S., Li, J., Gou, X., and Chen, D. (2016). Blocking mammalian target of rapamycin alleviates bladder hyperactivity and pain in rats with cystitis. Mol. Pain 12.
29. Wang, X., Li, X., Huang, B., and Ma, S. (2016). Blocking mammalian target of rapamycin (mTOR) improves neuropathic pain evoked by spinal cord injury. Transl. Neurosci. 7, 50–55.
30. Rabchevsky, A.G., Patel, S.P., Duale, H., Lyttle, T.S., O'Dell, C.R., and Kitzman, P.H. (2011). Gabapentin for spasticity and autonomic dysreflexia after severe spinal cord injury. Spinal Cord 49, 99–105.
31. Rabchevsky, A.G., Patel, S.P., Lyttle, T.S., Eldahan, K.C., O'Dell, C.R., Zhang, Y., Popovich, P.G., Kitzman, P.H., and Donohue, K.D. (2012). Effects of gabapentin on muscle spasticity and both induced as well as spontaneous autonomic dysreflexia after complete spinal cord injury. Front. Physiol. 3, 329.
32. Liu, G., Detloff, M.R., Miller, K.N., Santi, L., and Houle, J.D. (2012). Exercise modulates microRNAs that affect the PTEN/mTOR pathway in rats after spinal cord injury. Exp. Neurol. 233, 447–456.
33. Sun, Z., Hu, L., Wen, Y., Chen, K., Sun, Z., Yue, H., and Zhang, C. (2013). Adenosine triphosphate promotes locomotor recovery after spinal cord injury by activating mammalian target of rapamycin pathway in rats. Neural. Regen. Res. 8, 101–110.
34. Song, Y., Xue, H., Liu, T.T., Liu, J.M., and Chen, D. (2015). Rapamycin plays a neuroprotective effect after spinal cord injury via anti-inflammatory effects. J. Biochem. Mol Toxicol. 29, 29–34.
35. Zeng, L.H., Xu, L., Gutmann, D.H., and Wong, M. (2008). Rapamycin prevents epilepsy in a mouse model of tuberous sclerosis complex. Ann. Neurol. 63, 444–453.
36. Gassmann, M., Grenacher, B., Rohde, B., and Vogel, J. (2009). Quantifying Western blots: pitfalls of densitometry. Electrophoresis 30, 1845–1855.
37. Harlan, S.M., Guo, D.F., Morgan, D.A., Fernandes-Santos, C., and Rahmouni, K. (2013). Hypothalamic mTORC1 signaling controls sympathetic nerve activity and arterial pressure and mediates leptin effects. Cell Metab. 17, 599–606.

38. Obara, I., Tochiki, K.K., Geranton, S.M., Carr, F.B., Lumb, B.M., Liu, Q., and Hunt, S.P. (2011). Systemic inhibition of the mammalian target of rapamycin (mTOR) pathway reduces neuropathic pain in mice. Pain 152, 2582–2595.
39. Lu, Y., Inokuchi, H., McLachlan, E.M., Li, J.S., and Higashi, H. (2001). Correlation between electrophysiology and morphology of three groups of neuron in the dorsal commissural nucleus of lumbosacral spinal cord of mature rats studied in vitro. J. Comp. Neurol. 437, 156–169.
40. Matsushita, M. (1998). Ascending propriospinal afferents to area X (substantia grisea centralis) of the spinal cord in the rat. Exp. Brain Res. 119, 356–366.
41. Dragunow, M. and Faull, R. (1989). The use of c-fos as a metabolic marker in neuronal pathway tracing. J. Neurosci. Methods 29, 261–265.
42. Budde, K., Becker, T., Arns, W., Sommerer, C., Reinke, P., Eisenberger, U., Kramer, S., Fischer, W., Gschaidmeier, H., Pietruck, F., and ZEUS Study Investigators. (2011). Everolimus-based, calcineurin-inhibitor-free regimen in recipients of de-novo kidney transplants: an open-label, randomised, controlled trial. Lancet 377, 837–847.
43. McCormack, F.X., Inoue, Y., Moss, J., Singer, L.G., Strange, C., Nakata, K., Barker, A.F., Chapman, J.T., Brantly, M.L., Stocks, J.M., Brown, K.K., Lynch, J.P., 3rd, Goldberg, H.J., Young, L.R., Kinder, B.W., Downey, G.P., Sullivan, E.J., Colby, T.V., McKay, R.T., Cohen, M.M., Korbee, L., Taveira-DaSilva, A.M., Lee, H.S., Krischer, J.P., Trapnell, B.C., National Institutes of Health Rare Lung Diseases Consortium; MILS Trial Group. (2011). Efficacy and safety of sirolimus in lymphangioleiomyomatosis. N Engl J Med 364, 1595–1606.
44. Massard, C., Fizazi, K., Gross-Goupil, M., and Escudier, B. (2010). Reflex sympathetic dystrophy in patients with metastatic renal cell carcinoma treated with everolimus. Invest. New Drugs 28, 879–881.
45. Molina, M.G., Diekmann, F., Burgos, D., Cabello, M., Lopez, V., Oppenheimer, F., Navarro, A., and Campistol, J. (2008). Sympathetic dystrophy associated with sirolimus therapy. Transplantation 85, 290–292.
46. Melemedjian, O.K., Khoutorsky, A., Sorge, R.E., Yan, J., Asiedu, M.N., Valdez, A., Ghosh, S., Dussor, G., Mogil, J.S., Sonenberg, N., and Price, T.J. (2013). mTORC1 inhibition induces pain via IRS-1-dependent feedback activation of ERK. Pain 154, 1080–1091.
47. Karim, F., Wang, C.C., and Gereau, R.W. 4th (2001). Metabotropic glutamate receptor subtypes 1 and 5 are activators of extracellular signal-regulated kinase signaling required for inflammatory pain in mice. J. Neurosci. 21, 3771–3779.
48. Melemedjian, O.K., Asiedu, M.N., Tillu, D.V., Peebles, K.A., Yan, J., Ertz, N., Dussor, G.O., and Price, T.J. (2010). IL-6- and NGF-induced rapid control of protein synthesis and nociceptive plasticity via convergent signaling to the eIF4F complex. J. Neurosci. 30, 15113–15123.
49. Tateda, S., Kanno, H., Ozawa, H., Sekiguchi, A., Yahata, K., Yamaya, S., and Itoi, E. (2017). Rapamycin suppresses microglial activation and reduces the development of neuropathic pain after spinal cord injury. J Orthop. Res. 35, 93–103.
50. Sarbassov, D.D., Ali, S.M., Sengupta, S., Sheen, J.H., Hsu, P.P., Bagley, A.F., Markhard, A.L., and Sabatini, D.M. (2006). Prolonged rapamycin treatment inhibits mTORC2 assembly and Akt/PKB. Mol. Cell 22, 159–168.
51. Fang, Y., Westbrook, R., Hill, C., Boparai, R.K., Arum, O., Spong, A., Wang, F., Javors, M.A., Chen, J., Sun, L.Y., and Bartke, A. (2013). Duration of rapamycin treatment has differential effects on metabolism in mice. Cell Metab. 17, 456–462.
52. Furlan, J.C. and Fehlings, M.G. (2008). Cardiovascular complications after acute spinal cord injury: pathophysiology, diagnosis, and management. Neurosurg. Focus 25, E13.
53. Frankel, H.L., Michaelis, L.S., Golding, D.R., and Beral, V. (1972). The blood pressure in paraplegia. I. Paraplegia 10, 193–200.
54. Mayorov, D.N., Adams, M.A., and Krassioukov, A.V. (2001). Telemetric blood pressure monitoring in conscious rats before and after compression injury of spinal cord. J. Neurotrauma 18, 727–736.
55. Laird, A.S., Carrive, P., and Waite, P.M. (2006). Cardiovascular and temperature changes in spinal cord injured rats at rest and during autonomic dysreflexia. J. Physiol. 577, 539–548.
56. West, C.R., Popok, D., Crawford, M.A., and Krassioukov, A.V. (2015). Characterizing the temporal development of cardiovascular dysfunction in response to spinal cord injury. J. Neurotrauma 32, 922–930.
57. Mayet, J. and Hughes, A. (2003). Cardiac and vascular pathophysiology in hypertension. Heart 89, 1104–1109.
58. Sundaram, K., Murugaian, J., and Sapru, H. (1989). Cardiac responses to the microinjections of excitatory amino acids into the intermediolateral cell column of the rat spinal cord. Brain Res. 482, 12–22.
59. Martins, L., Fernandez-Mallo, D., Novelle, M.G., Vazquez, M.J., Tena-Sempere, M., Nogueiras, R., Lopez, M., and Dieguez, C. (2012). Hypothalamic mTOR signaling mediates the orexigenic action of ghrelin. PLoS One 7, e46923.
60. Deblon, N., Bourgoin, L., Veyrat-Durebex, C., Peyrou, M., Vinciguerra, M., Caillon, A., Maeder, C., Fournier, M., Montet, X., Rohner-Jeanrenaud, F., and Foti, M. (2012). Chronic mTOR inhibition by rapamycin induces muscle insulin resistance despite weight loss in rats. Br. J. Pharmacol. 165, 2325–2340.
61. Hebert, M., Licursi, M., Jensen, B., Baker, A., Milway, S., Malsbury, C., Grant, V.L., Adamec, R., Hirasawa, M., and Blundell, J. (2014). Single rapamycin administration induces prolonged downward shift in defended body weight in rats. PLoS One 9, e93691.
62. Cloughesy, T.F., Yoshimoto, K., Nghiemphu, P., Brown, K., Dang, J., Zhu, S., Hsueh, T., Chen, Y., Wang, W., Youngkin, D., Liau, L., Martin, N., Becker, D., Bergsneider, M., Lai, A., Green, R., Oglesby, T., Koleto, M., Trent, J., Horvath, S., Mischel, P.S., Mellinghoff, I.K., and Sawyers, C.L. (2008). Antitumor activity of rapamycin in a Phase I trial for patients with recurrent PTEN-deficient glioblastoma. PLoS Med 5, e8.
63. Crandall, D.L., Goldstein, B.M., Gabel, R.A., and Cervoni, P. (1984). Hemodynamic effects of weight reduction in the obese rat. Am. J. Physiol. 247, R266–R271.
64. Vincent, J.L. (2008). Understanding cardiac output. Crit. Care 12, 174.
65. Reis, F., Parada, B., Teixeira de Lemos, E., Garrido, P., Dias, A., Piloto, N., Baptista, S., Sereno, J., Eufrasio, P., Costa, E., Rocha-Pereira, P., Santos-Silva, A., Figueiredo, A., Mota, A., and Teixeira, F. (2009). Hypertension induced by immunosuppressive drugs: a comparative analysis between sirolimus and cyclosporine. Transplant. Proc. 41, 868–873.
66. Watts, S.W., Morrison, S.F., Davis, R.P., and Barman, S.M. (2012). Serotonin and blood pressure regulation. Pharmacol. Rev. 64, 359–388.
67. Sekiguchi, A., Kanno, H., Ozawa, H., Yamaya, S., and Itoi, E. (2012). Rapamycin promotes autophagy and reduces neural tissue damage and locomotor impairment after spinal cord injury in mice. J. Neurotrauma 29, 946–956.
68. Squair, J.W., West, C.R., Popok, D., Assinck, P., Liu, J., Tetzlaff, W., and Krassioukov, A.V. (2017). High thoracic contusion model for the investigation of cardiovascular function after spinal cord injury. J. Neurotrauma 34, 671–684.

Address correspondence to:
Alexander G. Rabchevsky, PhD
Spinal Cord and Brain Injury Research Center (SCoBIRC)
University of Kentucky
Biomedical and Biological Sciences Research Building, B471
741 South Limestone Street
Lexington, KY 40536-0509

E-mail: agrab@uky.edu